Infrared and Raman spectroscopy of Nd_2CuO_4-based superconductors

M. K. Crawford
E. I. du Pont de Nemours & Company, Central Research & Development Department, Experimental Station, Wilmington, Delaware 19880-0356

G. Burns, G. V. Chandrashekhar, and F. H. Dacol
IBM Research Division, Thomas J. Watson Research Center, Yorktown Heights, New York 10598-0218

W. E. Farneth, E. M. McCarron III, and R. J. Smalley
E. I. du Pont de Nemours & Company, Central Research & Development Department, Experimental Station, Wilmington, Delaware 19880-0356

(Received 20 November 1989)

We report infrared and Raman measurements of phonons in the recently discovered electron-doped superconductors $Nd_{2-x}(Ce,Th)_xCuO_4$, and undoped Nd_2CuO_4. Utilizing data from ceramics and *ab*-plane single crystals, we have identified all of the expected infrared-active modes ($3A_{2u}+4E_u$). We have also observed the Raman modes for motion along the *c* axis in the pure and doped materials. Based on our data and group theory, we assign the observed phonons. Finally, we compare the phonons in this class of materials to those of the related hole superconductors based upon La_2CuO_4.

INTRODUCTION

The T' structure in which Nd_2CuO_4 crystallizes has been known[1] since 1975. Interest in these materials has greatly increased since the discovery that they can be electron doped (*n* type), yielding metals which superconduct[2,3] with critical temperatures as high as 30 K. The T' structure of $Nd_{2-x}Ce_xCuO_4$ is similar to the T structure of the hole-doped (*p*-type) superconductor $La_{2-x}Sr_xCuO_4$. These two structures are shown[4] in Fig. 1 and are discussed below. In this paper we report the results of infrared and Raman measurements of the $Nd_{2-x}(Ce,Th)_xCuO_4$ system. These results will be useful for comparison to lattice dynamical calculations and inelastic neutron scattering phonon dispersion curves when they become available.

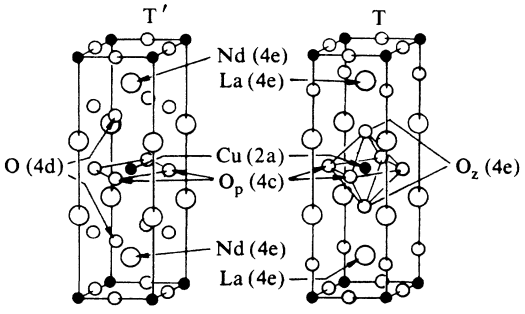

FIG. 1. Unit cells of the tetragonal T' and T structures, as labeled. The atoms are labeled using the Wyckoff notation.

EXPERIMENT

Crystals of Nd_2CuO_4, $Nd_{2-x}Ce_xCuO_4$, and $Nd_{2-x}Th_xCuO_4$ were grown by slow cooling of melts containing an excess of CuO. The compounds were formed by mixing the ingredient oxides or carbonates in stoichiometric proportions and heating to 1000 °C for 24 h, then grinding and reheating to 1000 °C for an overnight period. The compounds were then mixed with CuO in a 1:3.5 mole ratio in a Pt crucible, raised to 1300 °C at 200 °C/h, held there for up to 4 h, slow cooled at a rate of 1–2 °C/h to 850 °C, and then furnace cooled to room temperature. The crystals tend to grow in cavities and can be mechanically separated. Crystals 4 mm^2 in area and 0.2 mm thick have been obtained. Their composition was determined by electron microprobe analysis. The single crystals as grown were not superconducting, although they have the T' structure as shown by powder x-ray diffraction.

$Nd_{2-x}Ce_xCuO_4$ ceramics were prepared by standard solid-state techniques using stoichiometric (for $x=0.15$) quantities of Nd_2O_3, CeO_2, and CuO. Well-ground mixtures of the binary oxides were fired to 1100 °C in air for 12 h. The samples were reground and refired under the same conditions to ensure complete reaction. Phase purity was checked by powder x-ray diffraction and all detected lines were indexed. Superconductivity was achieved by annealing the samples at 900 °C in nitrogen for 12 h. A typical $Nd_{1.85}Ce_{0.15}CuO_4$ sample exhibited a T_c onset of 16.5 K and a 10% Meissner fraction. Experimental details of the infrared[5] and Raman[6] measurements have been described previously.

RESULTS AND DISCUSSION

Both the T and T' structures are body-centered tetragonal, space group $14/mmm\text{-}D_{4h}^{17}$, and most of the corresponding atoms in the two chemical formulas occupy the same Wyckoff positions,[4] as can be seen in Fig. 1. Both structures have two formula units in a body-centered tetragonal unit cell, or one formula unit per primitive unit cell. They each also have a single Cu-O plane, made up of one Cu($2a$) and two O_p($4c$) atoms, per primitive unit cell (O_p refers to O on the plane), and Nd/La at the $4e$ site.[4] The difference between the structures arises from the position of the other two oxygen atoms. The T structure has an oxygen atom, O_z, at the Wyckoff $4e$ position, which is directly (along the z axis) above and below the Cu atoms. In the T' structure, however, the additional oxygen atom is at the Wyckoff $4d$ position (Fig. 1). The O($4d$) atom is not chemically bonded to Cu($2a$). This difference leads to a change in the group theoretical classification of the phonons in the T' structure compared to the T structure and modifies the phonon eigenvectors.

In Table I we list the phonon symmetries for each atom in both the T and T' structures.[7] In the T structure both the La and the O_z($4e$) atoms can vibrate in the A_{1g} modes. In the T' structure, however, only the Nd atoms move in the A_{1g} mode, whereas only the O($4d$) atoms contribute to the eigenvector for the B_{1g} mode. This is an exact result dictated by symmetry and constitutes an important distinction for Raman spectroscopy of the two structures. The E_g modes, on the other hand, involve motion of La plus O_z($4e$) in the T structure or Nd plus O($4d$) in the T' structure but, due to the differences in chemical bonding, the phonon eigenvectors and energies in the two structures may not be the same. Finally, it should be noted that neither the Cu nor O atoms in the Cu-O sheets participate in Raman-active vibrations in the T or T' structures.

The infrared active phonons in the two structures are similar in that one expects to observe $3A_{2u}+4E_u$ phonons in either case. The differences in chemical bonding and unit cell dimensions should, however, lead to differences in eigenvectors, frequencies, and oscillator strengths for the phonons in the two structures.

Unlike the situation[8] in insulating $YBa_2Cu_3O_6$, the

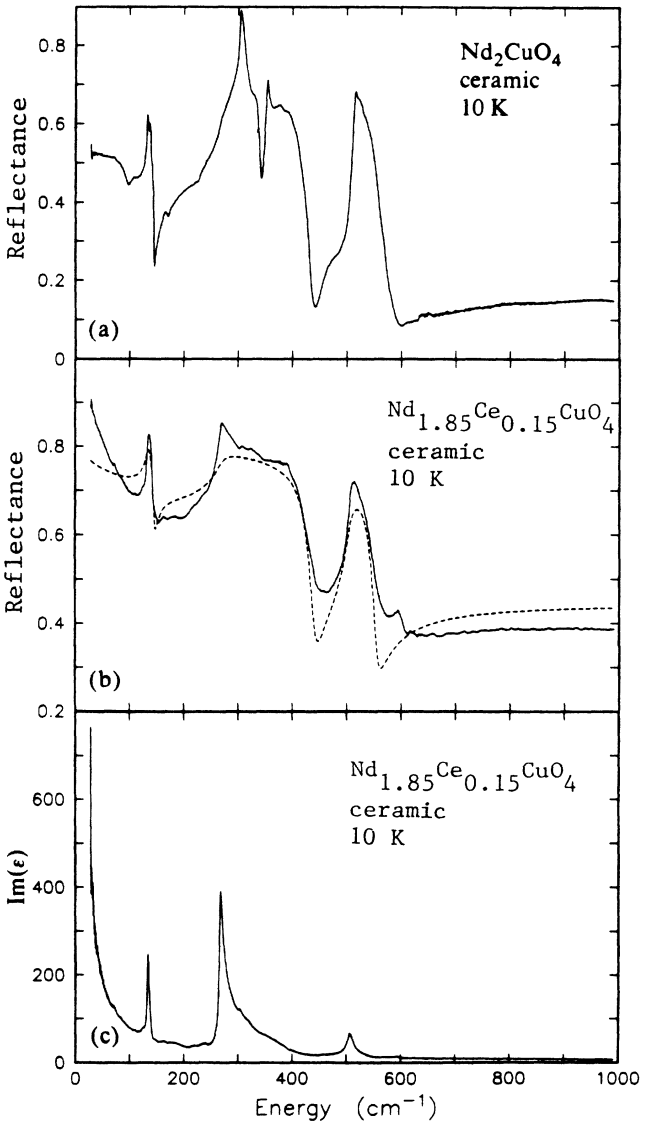

FIG. 2. Results for Nd_2CuO_4. (a) Reflectance from an insulating ceramic. All the infrared modes are observed. (b) Reflectance from an electron doped ceramic. The three A_{2u} modes and an ab-plane plasma are observed. The dashed line is the fit. (The parameters used are $\epsilon_\infty=25$, $\omega_{\text{plasma}}=2000$ cm^{-1}, and $\gamma_{\text{plasma}}=8000$ cm^{-1}.) (c) The Kramers-Kronig analysis of the doped ceramic reflectance.

TABLE I. Classification of phonons in tetragonal La_2CuO_4 (T structure) and Nd_2CuO_4 (T' structure) (Ref. 7). Both structures have space group $I4/mmm\text{-}D_{4h}^{17}$.

T structure		T' structure	
Mode symmetries	Atom	Atom	Mode symmetries
$A_{2u}+E_u$	Cu($2a$)	Cu($2a$)	$A_{2u}+E_u$
$A_{2u}+B_{2u}+2E_u$	O_p($4c$)	O_p($4c$)	$A_{2u}+B_{2u}+2E_u$
$A_{2u}+E_u+A_{1g}+E_g$	O_z($4e$)	O($4d$)	$A_{2u}+E_u+B_{1g}+E_g$
$A_{2u}+E_u+A_{1g}+E_g$	La($4e$)	Nd($4e$)	$A_{2u}+E_u+A_{1g}+E_g$
Sum of modes grouped according to activity:			
Acoustic	$A_{2u}+E_u$	$A_{2u}+E_u$	
Infrared	$3A_{2u}+4E_u$	$3A_{2u}+4E_u$	
Raman	$2A_{1g}+2E_g$	A_{1g} (only Nd)$+B_{1g}$ [only O($4d$)]$+2E_g$	
Silent	B_{2u} [O_p($4c$) only]	B_{2u} [O_p($4c$) only]	

TABLE II. TO and LO phonon energies, ω_{TO} and ω_{LO} (cm^{-1}), and damping, γ (cm^{-1}, $\gamma_{TO}=\gamma_{LO}$), for Nd_2CuO_4 at 10 K. Values of ω_{TO} are the energies at which the maxima in $\mathrm{Im}(\epsilon)$ occur. The oscillator strengths, S_i, are obtained from the expression $\epsilon=\epsilon_\infty[1+\Sigma_i S_i\omega_{TO,i}^2/(\omega_{TO,i}^2-\omega^2)]$.

Symmetry	ω_{TO}	ω_{LO}	γ	S_i
A_{2u}	134	146	7	0.739
A_{2u}	269	440	20	2.028
A_{2u}	505	555	15	0.069
E_u	129	140	9	0.557
E_u	300	342	11	1.395
E_u	350	437	12	0.157
E_u	509	595	17	0.152

infrared-active phonons of A_{2u} and E_u symmetry in Nd_2CuO_4 (and La_2CuO_4) overlap in energy, making phonon assignments based only upon ceramic data difficult. Therefore, single crystal measurements are required in order to separate modes of different symmetry. Platelike single crystals allow observation of the *ab*-plane E_u phonons, but not the *c* axis polarized A_{2u} modes. However, another technique may be employed to separate the A_{2u} and E_u modes in ceramics. By doping the materials with free charge carriers, we can effectively screen the in-plane E_u modes, allowing us to observe only the A_{2u} modes in the ceramics. Any *c*-axis plasma response in these materials is at a low frequency and does not significantly affect the A_{2u} modes. We note that the A_{2u} TO phonon energies so determined might be slightly shifted compared to what one would obtain in an undoped single crystal measurement.

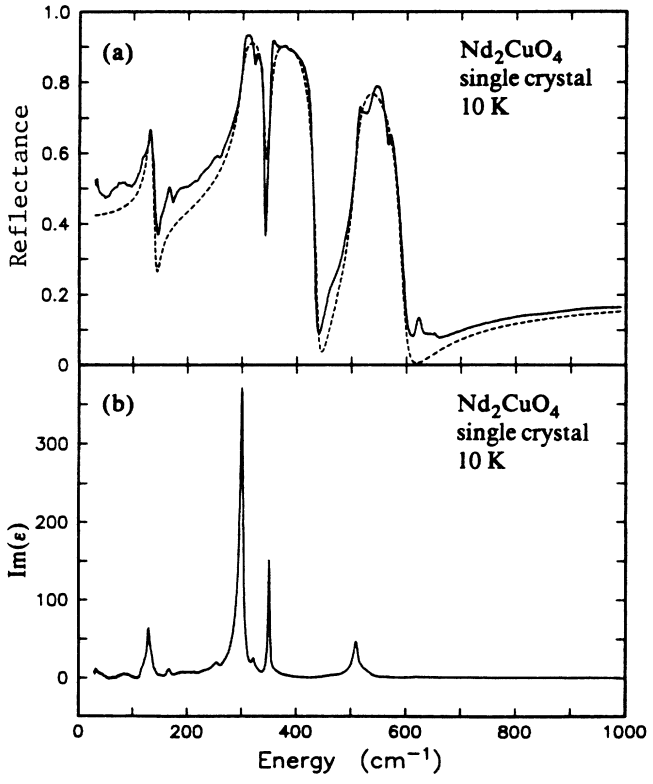

FIG. 3. (a) The infrared reflectance from a small *ab*-plane Nd_2CuO_4 insulating single crystal. The dashed line is the fit. ($\epsilon_\infty=6.8$ was used.) (b) The Kramers-Kronig analysis of the single crystal reflectance.

In Fig. 2(a) we show the infrared reflectance from ceramic semiconducting (undoped) Nd_2CuO_4. It is not obvious how to assign phonons or, in fact, how many phonons are present. In Fig. 2(b) we show the reflectance of Ce-doped Nd_2CuO_4 ($Nd_{1.85}Ce_{0.15}CuO_4$). As can be seen, the spectra simplify, revealing three reststrahlen bands. This simplification occurs because the $4E_u$ modes are screened and thus the expected $3A_{2u}$ phonon reststrahlen bands are observed. These three bands are superimposed on a free carrier background from the now conducting *ab*-plane. The theoretical fit[9] is also shown in Fig. 2(b). We did not include a *c* axis plasma contribution in the fit. Figure 2(c) shows $\mathrm{Im}(\epsilon)$, yielding the transverse-optic (TO) phonon energies which are used in the fit (Table II).

The assignments of the $3A_{2u}$ modes (vibration along the *c* axis) are as follows. The 134 cm^{-1} mode is primarily the heavy atom Nd vibration, the 269 cm^{-1} phonon is the Cu-O sheet bending mode, and the 505 cm^{-1} phonon is the O(4*d*) mode. The $3A_{2u}$ modes in Pr_2CuO_4 occur at similar energies.[10]

In Fig. 3(a) we show the infrared reflectance of the *ab* plane of a single crystal of Nd_2CuO_4. There are clearly four dominant phonons corresponding to the $4E_u$ modes expected. $\mathrm{Im}(\epsilon)$, determined by a Kramers-Kronig analysis, is shown in Fig. 3(b) and yields the TO mode energies (Table II) which are used in the oscillator fit. The dashed line in Fig. 3(a) is the oscillator fit which also yields the LO modes (Table II).

The assignments of the $4E_u$ modes (doubly degenerate vibrations in the *ab* plane) can be made as follows. The TO phonon at 129 cm^{-1} is the Nd E_u mode. The TO mode at 300 cm^{-1} is the Cu-O sheet bending mode, whereas the 350 cm^{-1} phonon can be assigned as the O(4*d*) E_u phonon. The latter assignments are based upon our observation that the 300 cm^{-1} phonon in Nd_2CuO_4 also appears[10] at 300 cm^{-1} in Pr_2CuO_4, whereas the 350 cm^{-1} phonon in Nd_2CuO_4 has shifted to 336 cm^{-1} in Pr_2CuO_4, presumably due to a change in the Ln-O(4*d*) force constant. We assign the highest frequency E_u mode at 509 cm^{-1} in Nd_2CuO_4 to the Cu-O in-plane stretching vibration.

We note that the spectra [Figs. 2(b) and 3(a)] exhibit small scale structure for which we have no conclusive explanation at present. The samples appear single phase by

TABLE III. Comparison of TO phonon energies in Nd_2CuO_4 and La_2CuO_4.

	A_{2u}			E_u			
Nd_2CuO_4	134	269	505	129	300	350	509
La_2CuO_4[a]	242	342	501	132	358		667

[a]Data taken from Ref. 11.

TABLE IV. Energies of the A_{1g} Raman modes in various single crystals with the T' structure. The mode is observed in (zz) polarization and the energies are given in cm^{-1}.

Nd_2CuO_4	$Nd_{1.84}Ce_{0.16}CuO_4$	$Nd_{1.85}Th_{0.15}CuO_4$	$Nd_{1.83}Sr_{0.17}CuO_4$
228.2	229	228	229

x-ray diffraction, so impurities do not offer a likely explanation. The *ab* plane mosaics appeared well oriented by Laue diffraction; thus, *c*-axis spectral contamination is unlikely. It is possible that the actual crystal symmetry is lower than $I4/mmm$ at 10 K (i.e., that a low-temperature phase transition occurs), or that some disorder-induced effects are present due, for example, to oxygen nonstoichiometry.

In Table III we compare the phonon energies observed in Nd_2CuO_4 (T' structure) with those in La_2CuO_4 (T structure).[11] In general, the phonon energies in Nd_2CuO_4 are lower than in La_2CuO_4. This is primarily a result of the larger unit cell dimensions (and therefore longer bond lengths) in the former material. Phonons with similar eigenvectors will thus have higher energies in La_2CuO_4. (In general, the eigenvectors for the phonons in the two materials will be different, since the bonding arrangements are different.) In Nd_2CuO_4 (and La_2CuO_4, Ref. 11) the phonons with the largest oscillator strength (Table II) are the 300 cm^{-1} Cu-O E_u bond bending mode and the 269 cm^{-1} A_{2u} Cu-O bond bending mode. The phonon oscillator strengths, and therefore the effective ionic charges, are similar in the two materials.

A fairly complete paper on the Raman modes in pure Nd_2CuO_4 single crystals has been published.[12] At 30 K he observes the A_{1g} (230 cm^{-1}), B_{1g} (344 cm^{-1}), and one of the two E_g (494 cm^{-1}) allowed modes (Table I). In Nd_2CuO_4 single crystals at room temperature we have observed the latter two modes at 333 and 488 cm^{-1}.

We have also observed the A_{1g} mode in a variety of small single crystals and the results are given in Table IV. As can be seen, the phonon frequency is fairly independent of doping, despite the different masses of the dopant ions. (For Pr_2CuO_4 we observe this mode at 230 cm^{-1}.) This is somewhat surprising and may indicate "two-mode" behavior for different atoms in this site, although we have not observed a new mode at these dopant levels. The A_{1g} mode is allowed in (zz) and (xx) polarizations, but we find that the (zz) intensity can be greater than 60 times that in (xx). For a mode just involving Nd atom motion, this is surprising. We also note that this mode is at essentially the same frequency as a similar mode in La_2CuO_4 (230 cm^{-1}), although in the latter material symmetry allows some $O_z(4e)$ atom motion as well as La motion (Fig. 1).

For some crystals, in (zz) polarization, we also observe a Raman feature at about 590 cm^{-1}. This is similar to the feature observed by Sugai[12] in (xy) polarization. There is a tendency to suggest that such features are infrared active TO (or LO) phonons made Raman active by disorder. This conjecture is difficult to prove, but this feature, only observed in some crystals, is close to the E_u(LO) mode at 595 cm^{-1} (Table II). Comparison of the ^{18}O isotope shifts for the Raman and infrared modes will enable us to determine if they have the same eigenvector.

CONCLUSIONS

In conclusion, we have reported the results of infrared and Raman measurements of phonons in materials having the T' structure. We have identified all of the $(3A_{2u}+4E_u)$ infrared-active phonons predicted by group theory and have observed the Raman-active vibrations involving atomic motion parallel to the *c* axis. In addition, we have given assignments for the observed phonons.

ACKNOWLEDGMENTS

The authors wish to thank W. Dolinger and M. W. Sweeten for their excellent technical assistance.

[1]H. Müller-Buschbaum and W. Wollschläger, Z. Anorg. Allg. Chem. **414**, 76 (1975).

[2]Y. Tokura, H. Takagi, and S. Uchida, Nature **337**, 345 (1989).

[3]H. Takagi, S. Uchida, and Y. Tokura, Phys. Rev. Lett. **62**, 1197 (1989).

[4]G. Burns and A. M. Glazer, *Space Groups for Solid State Scientists* (Academic, New York, 1990).

[5]M. K. Crawford, W. E. Farneth, E. M. McCarron III, and R. K. Bordia, Phys. Rev. B **38**, 11 382 (1988).

[6]G. Burns, F. H. Dacol, and M. W. Shafer, Solid State Commun. **62**, 687 (1987); G. Burns, F. H. Dacol, G. Klich, W. König, and M. W. Shafer, Phys. Rev. B **37**, 3381 (1988).

[7]G. Burns, M. K. Crawford, F. H. Dacol, E. M. McCarron III, and T. M. Shaw, Phys. Rev. B **40**, 6717 (1989).

[8]M. K. Crawford, G. Burns, and F. Holtzberg, Solid State Commun. **70**, 557 (1989).

[9]F. Wooten, *Optical Properties of Solids* (Academic, New York, 1972). The various equations can be found in Chap. 3 and the factorized phonon part in Ref. 7.

[10]M. K. Crawford, G. Burns, G. V. Chandrashekhar, F. H. Dacol, W. E. Farneth, E. M. McCarron III, and R. J. Smalley, Solid State Commun. **73**, 507 (1990).

[11]R. T. Collins, Z. Schlesinger, G. V. Chandrashekhar, and M. W. Shafer, Phys. Rev. B **39**, 2251 (1989).

[12]S. Sugai, T. Kobayashi, and J. Akimitsu, Phys. Rev. B **40**, 2686 (1989); E. T. Heyer, R. Liu, B. Gegenheimer, C. Thomsen, and M. Cardona (unpublished).